

## Shape Selection in the Association of Diaminoguanidinium Cation with Counterions<sup>†</sup>

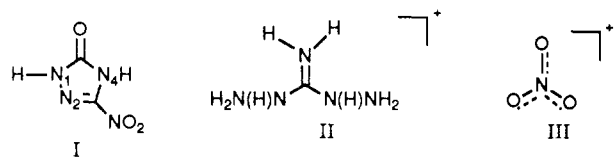
James P. Ritchie,\* K.-Y. Lee, D. T. Cromer, E. M. Kober, and D. D. Lee

Los Alamos National Laboratory, Los Alamos, New Mexico 87545

Received September 5, 1989

X-ray crystal structure determination shows that the conformation of the diaminoguanidinium (DAG) cation  $((\text{NH}_2\text{NH})_2\text{C}=\text{NH}_2)^+$  is different in its salts with nitrate ion and with the conjugate base of 3-nitro-1,2,4-triazol-5-one (NTO). In both cases, the carbon atom and all five nitrogen atoms are coplanar. In the nitrate salt an "S" configuration is found where one of the terminal  $\text{NH}_2$  groups is cis to the central  $\text{C}=\text{NH}_2$  bond and the other is trans. In the NTO salt a "W" configuration is found where both of the terminal  $\text{NH}_2$  groups are cis to the central  $\text{C}=\text{NH}_2$  bond. The terminal  $\text{NH}_2$  groups are positioned in such a fashion that the hydrogens appear above and below the plane of the molecule and the lone pairs are directed toward the hydrogens of the  $\text{C}=\text{NH}_2$  moiety. AM1 calculations were performed for a variety of DAG conformations to give a qualitative indication of the relative energies. The S and W forms were not found to be true minima by this method because of a spurious tendency toward pyramidalization of the "guanidine" nitrogens. Ab initio molecular orbital calculations, however, show that both the S and W forms are potential energy minima in the absence of counterions, and that the S form is the more stable by about 0.5 kcal/mol. Other forms for the DAG cation were calculated, but were found to be higher in energy. Topological analysis of the S and W forms shows unusual N-N bond paths, rather than N-H bond paths expected for "typical" hydrogen bonds. Additionally, integrated populations are used to assess "Y" delocalization of charge. Energies of the complexes formed by the NTO conjugate base with the W and S forms of DAG were calculated using an electrostatic model. The association energies showed that the W form is complexed more strongly than the S form. The difference in this energy is larger and oppositely signed from the W/S energy difference as "free" cations. Thus, the calculations suggest that the nitrate salt contains DAG in its lower energy form, while favorable electrostatic interactions lead to selective binding of the less stable W form of DAG with NTO.

Interest in 3-nitro-1,2,4-triazol-5-one (NTO, I) as a less sensitive explosive<sup>1</sup> led us to prepare its diaminoguanidinium (DAG, II) salt as a possible chemical propellant. The crystal structure of this salt (called DAGNTO) was recently determined by X-ray analysis<sup>2</sup> and, to the best of our knowledge, is the first of a diaminoguanidinium salt. Previous molecular orbital calculations showed I to be the most stable tautomer of NTO and that deprotonation at the 4-position leads to the most stable conjugate base.<sup>3</sup> In this paper, we report the crystal structure of the nitrate (III) salt of DAG. The resulting



salt (called DAGNIT) has been previously prepared,<sup>4</sup> but by a different method. Comparison of the DAG geometry in these two salts shows it is in different conformations. Thus, one of the counterions is selectively binding with the less stable conformer of the DAG cation, a simple case of "molecular recognition",<sup>5</sup> unless the conformers are accidentally degenerate in energy. Because of the tremendous interest in this area and our own interests in understanding crystal structures, we performed a number of calculations to determine the factor likely to account for this observation. This paper describes the results of these investigations.

### Methods

**Experimental.** Diaminoguanidinium nitrate was prepared by passing a solution of diaminoguanidine hydrochloride (Aldrich) through a column of Amberlite IRA-400 ( $\text{OH}^-$  form) to release the free DAG base and mixing it immediately with an equimolar aqueous solution of nitric

acid. Colorless crystals for X-ray diffraction crystallized from water and ethanol. Selected crystal, ca.  $0.25 \times 0.15 \times 0.06$  mm. CAD-4 diffractometer,  $\theta - 2\theta$  scan. Scan range,  $0.9 + 0.34 \tan \theta$  deg. Scan speed, 0.9-5.5 deg/min. Background first and last 1/6 of scan. Graphite monochromated  $\text{Mo K}\alpha$  radiation. Unit cell, 25 reflections  $13^\circ < \theta < 21^\circ$ . No absorption corrections.  $\text{Sin } \theta / \lambda_{\text{max}} = 0.596 \text{ \AA}^{-1}$ . Index range  $0 \leq h \leq 7, -8 \leq k \leq 8, -8 \leq l \leq 8$ , 1209 reflections measured and averaged to yield 1093 unique reflections, of which 850 were observed with  $I > 2\sigma(I)$ ,  $R_f = 0.011$ . Standard reflections 322 and 033 showed no significant variation. Least squares minimized  $\sum w(\Delta F)^2$  with  $w = [\sigma_c^2(F) + 0.03F^2]^{-1}$ ,  $\sigma_c^2(F)$  based on counting statistics. Structure was solved by MULTAN,<sup>6</sup> hydrogens by difference Fourier. Scale factor, isotropic type II extinction parameter,<sup>7</sup> positional parameters, anisotropic thermal parameters for C, N, and O, and isotropic thermal parameters for H were refined. Final  $R = 0.028$ ,  $R_w = 0.078$ ,  $S = 1.85$ . Max.  $\sigma/\Delta = 0.0002$ . Final  $\Delta F$  Fourier synthesis  $-0.16 < \Delta\rho < 0.14$  electrons/ $\text{\AA}^3$ . Scattering factors  $f$  (RHF for C, N, O, and SDS for H),  $f', f''$  from standard source.<sup>8</sup> Calculations on CRAY-1 using the Los Alamos Crystal Structure System developed primarily by A. C. Larson.<sup>9</sup>

(1) (a) Lee, K.-Y.; Coburn, M. D. 3-Nitro-1,2,4-Triazol-5-one, A Less Sensitive Explosive U.S. Patent 4, 1988, 733, 610. (b) Lee, K.-Y.; Chapman, L. B.; Coburn, M. J. *Energetic Materials* 1987, 5, 27.

(2) Cromer, D. T.; Hall, J. H.; Lee, K.-Y.; Ryan, R. R. *Acta Crystallogr.* 1988, C44, 2206.

(3) Ritchie, J. P. *J. Org. Chem.* 1989, 54, 3553.

(4) Stevens, M. F. G. *J. Chem. Soc., Perkin Trans. 1* 1972, 1221 and references therein.

(5) (a) Cram, D. J. *Science (Washington, D.C.)* 1980, 240, 760. (b) Lehn, J. M. *Angew. Chem., Int. Ed. Engl.* 1988, 27, 89. (c) Pedersen, C. J. *Pure Appl. Chem.* 1988, 60, 450.

(6) Germain, G.; Main, P.; Woolfson, M. M. *Acta Crystallogr.* 1971, A27, 368.

(7) Larson, A. C. *Crystallographic Computing*; Ahmed, F. R., Ed.; Munksgaard: Copenhagen, 1969; p 291.

(8) *International Tables for X-ray Crystallography*; Kynoch Press: Birmingham, 1974; Vol. IV.

(9) Lists of structure factors, anisotropic thermal parameters, H atom parameters, and bond distances and angles involving H atoms are available as supplementary material.

<sup>†</sup> This research was jointly funded by the U.S. Department of Defense, Office of Munitions, and Department of Energy.

**Theoretical.** AM1 calculations were performed using the MOPAC program.<sup>10</sup> The GAUSSIAN-82 package was used for ab initio calculations<sup>11</sup> and standard basis sets were used throughout.<sup>12</sup> Geometries were completely optimized within stated symmetry groups unless noted otherwise. For selected species, atom-centered multipole expansions (ACME's) were obtained by integrating the electron density assigned to each atom using the Hirshfeld technique.<sup>13</sup> We have previously shown that ACME's calculated in this way and including up to the octupole terms accurately reproduce the electrostatic potentials calculated rigorously, provided the atoms are not approached more closely than their van der Waals radius.<sup>14</sup>

The total electrostatic interaction energy,  $E_{\text{ele}}$ , between two molecules, A and B, can be simply expressed by the multipole-multipole interactions of these ACME's as shown in eq 1.<sup>15</sup> Here, the multipole moments (charge, dipole, etc.) of atom  $i$  are  $q_i$ ,  $\mu_i$ , etc., and  $\vec{R}_{ij}$  is the distance vector between atoms  $i$  and  $j$ . The calculations here in-

$$E_{\text{ele}} = \sum_{i \in A} \sum_{j \in B} \frac{q_i q_j}{|\vec{R}_{ij}|} + \frac{q_i (\vec{\mu}_j \cdot \vec{R}_{ij})}{|\vec{R}_{ij}|^3} + \frac{q_j (\vec{\mu}_i \cdot \vec{R}_{ij})}{|\vec{R}_{ij}|^3} \dots \quad (1)$$

cluded up to octupole-octupole interactions. To represent the exchange-repulsion interaction, the atoms were essentially treated as hard spheres with standard "van der Waals" radii.<sup>16</sup> Because using true hard spheres caused significant problems in the geometry optimization, the spheres were softened somewhat by the use of an exponential repulsive term, which is given by the second term on the rhs of eq 2. Here,  $r_i$  and  $r_j$  are the van der Waals

$$E_{\text{TOT}} = E_{\text{ele}} + \sum_{i \in A} \sum_{j \in B} C e^{-D(r_i + r_j - R_{ij})} \quad (2)$$

radii of atoms  $i$  and  $j$ , and  $R_{ij}$  is the distance between those two atoms.  $C$  and  $D$  are somewhat arbitrary constants whose values ( $C = 0.0003$  hartree,  $D = 20/\text{bohr}$ ) were chosen so that the distance between two atoms "in contact" would be equal to the sum of the van der Waals radii  $\bullet$  0.02 Å. We emphasize that this term is not meant to be a realistic representation of the true exchange-repulsion energy, but is used only to soften the atomic spheres so that the geometry optimization could proceed smoothly. The total energy of interaction between the two molecules,  $E_{\text{TOT}}$ , is taken to be simply the sum of  $E_{\text{ele}}$  and this repulsive term (which is typically equal to 1% of  $E_{\text{ele}}$ ). The value of  $E_{\text{TOT}}$  was then minimized by standard procedures to find the optimal geometric arrangements. Since many local minima exist, numerous different starting positions and chemical intuition were used to infer that a true global minima had been found. Further details and applications of this model are described elsewhere.<sup>17</sup> This approach is very similar to that of Buckingham and Stone who use a model based on distributed multipole expansions (DME's).<sup>18</sup> Their results and ours show that this type of

(10) Dewar, M. J. S.; Zoebisch, E. G.; Healy, E. F.; Stewart, J. J. P. *J. Am. Chem. Soc.* **1985**, *107*, 3902. The authors thank Dr. Stewart for a copy of his program.

(11) Binkley, J. S.; Frisch, M. J.; DeFrees, D. J.; Ragavachari, K.; Whiteside, R. A.; Schlegel, H. B.; Fluder, E. M.; Pople, J. A.; Carnegie-Mellon University. The CTSS version was implemented by Dr. R. Martin, Los Alamos.

(12) 3-21G: Binkley, J. S.; Pople, J. A.; Hehre, W. J. *J. Am. Chem. Soc.* **1980**, *102*, 939. 6-31G+: Clark, T.; Chandrasekhar, J.; Spitznagel, G. W.; Schleyer, P. v. R. *J. Comput. Chem.* **1983**, *4*, 294. 6-31G\*: Hariharan, P. C.; Pople, J. A. *Theoret. Chem. Acta (Berl.)* **1973**, *28*, 213.

(13) Hirshfeld, F. L. *Theor. Chem. Acta* **1977**, *49*, 129.

(14) Ritchie, J. P. *J. Am. Chem. Soc.* **1985**, *107*, 1829.

(15) Buckingham, A. D. *Intermolecular Interactions: From Diatomics to Biopolymers*; Pullman, B., Ed.; Wiley: New York, 1978; Chapter 1.

(16) Bondi, A. J. *Phys. Chem.* **1964**, *68*, 441.

(17) Kober, E. M.; Ritchie, J. P.; Lee, D. D., manuscript in preparation.

**Table I. Summary of Crystallographic Data for Diaminoguanidinium Nitrate<sup>a</sup>**

molecular formula, CH <sub>8</sub> N <sub>6</sub> O <sub>3</sub> ; molecular weight, 152.11; space group, P $\bar{1}$				
lattice constants: $\lambda$ (Mo K $\alpha_1$ ) = 0.709 26 Å, $\mu$ = 1.39 cm <sup>-1</sup> , $F(000)$ = 160, $T$ = ~25 °C, $a$ = 6.039 (1) Å, $b$ = 6.972 (3) Å, $c$ = 7.764 (3) Å, $\alpha$ = 97.35 (3), $\beta$ = 96.58 (2), $\gamma$ = 102.14 (2)°, $V$ = 313.6 Å <sup>3</sup> , $Z$ = 2, $D_x$ = 1.611 mg m <sup>-3</sup>				
final $R$ = 0.028 for 850 obsd reflections $I > 2\sigma(I)$ out of 1093 independent reflections				
final least-squares parameters for the C, N, and O atoms; positional parameters $\times 10^4$ ; equivalent isotropic $U \times 10^2$ , $U = \frac{1}{3} \sum U_{ii}$				
atom	x	y	z	$U, \text{Å}^2$
Diaminoguanidinium Cation				
C	4550 (3)	7376 (2)	0589 (2)	2.8 (1)
N(1)	3647 (3)	6923 (3)	-2485 (2)	3.9 (2)
N(2)	3028 (3)	6628 (2)	-0830 (2)	3.2 (1)
N(3)	6650 (3)	8313 (2)	0445 (2)	3.8 (2)
N(4)	3986 (2)	7134 (2)	2161 (2)	3.6 (1)
N(5)	1683 (3)	6280 (3)	2298 (2)	3.9 (2)
Nitrate Anion				
N(6)	1753 (2)	1495 (2)	4091 (2)	3.3 (1)
O(1)	2661 (2)	0389 (2)	4926 (2)	4.6 (1)
O(2)	1777 (3)	3201 (2)	4803 (2)	5.5 (2)
O(3)	0802 (2)	0900 (2)	2551 (1)	4.6 (1)

<sup>a</sup>Type II isotropic extinction parameter =  $4.8 (1) \times 10^{-5}$  mm (Larson, A. C. *Crystallographic Computing*; Ahmed, F. R., Ed.; Munksgaard: Copenhagen, 1969; pp 291-296).

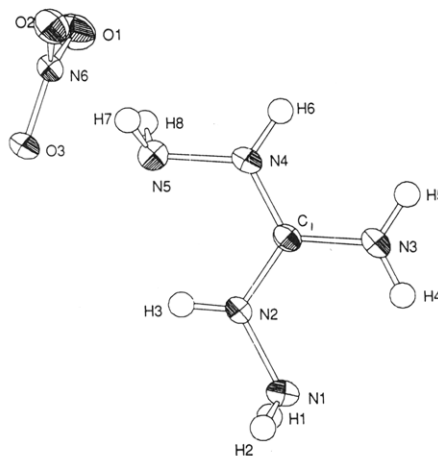


**Figure 1.** ORTEP drawing of the asymmetric unit of diaminoguanidinium nitrate. The numbering scheme reflects crystallographic conventions, resulting in differences from Chart I. Thermal ellipsoids are 30% probability. Hydrogen atoms are arbitrarily sized.

approach can often reliably predict the geometry and energy of interaction of so called "van der Waals" dimers, especially those involving hydrogen bonding.

Topological analysis and integration of the electron density for the "S" and "W" forms were performed using Bader's programs.<sup>19</sup>

## Results

**Crystal Structure.** Unit cell parameters and coordinates of the asymmetric unit for DAGNIT are shown in Table I, while Figure 1 shows an ORTEP plot of the atoms

(18) (a) Buckingham, A. D.; Fowler, P. W.; Stone, A. J. *Int. Rev. Phys. Chem.* **1986**, *5*, 107. (b) Buckingham, A. D.; Fowler, P. W. *Can. J. Chem.* **1985**, *65*, 2018. (c) Price, S. L.; Stone, A. J.; Alderton, M. *Mol. Phys.* **1984**, *52*, 987.

(19) Bregler-Konig, F. W.; Bader, R. F. W.; Tang, T.-H. *J. Comput. Chem.* **1982**, *3*, 317. The authors thank Professor Bader for supplying a copy of his program.

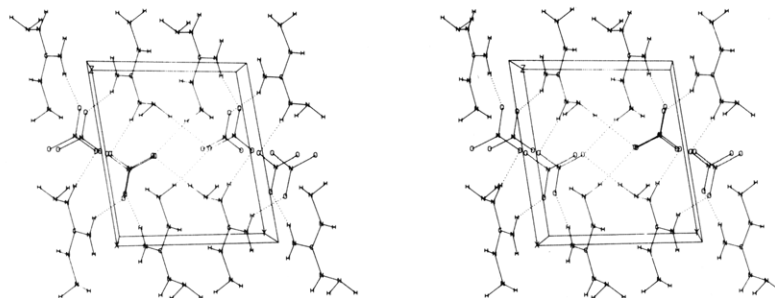
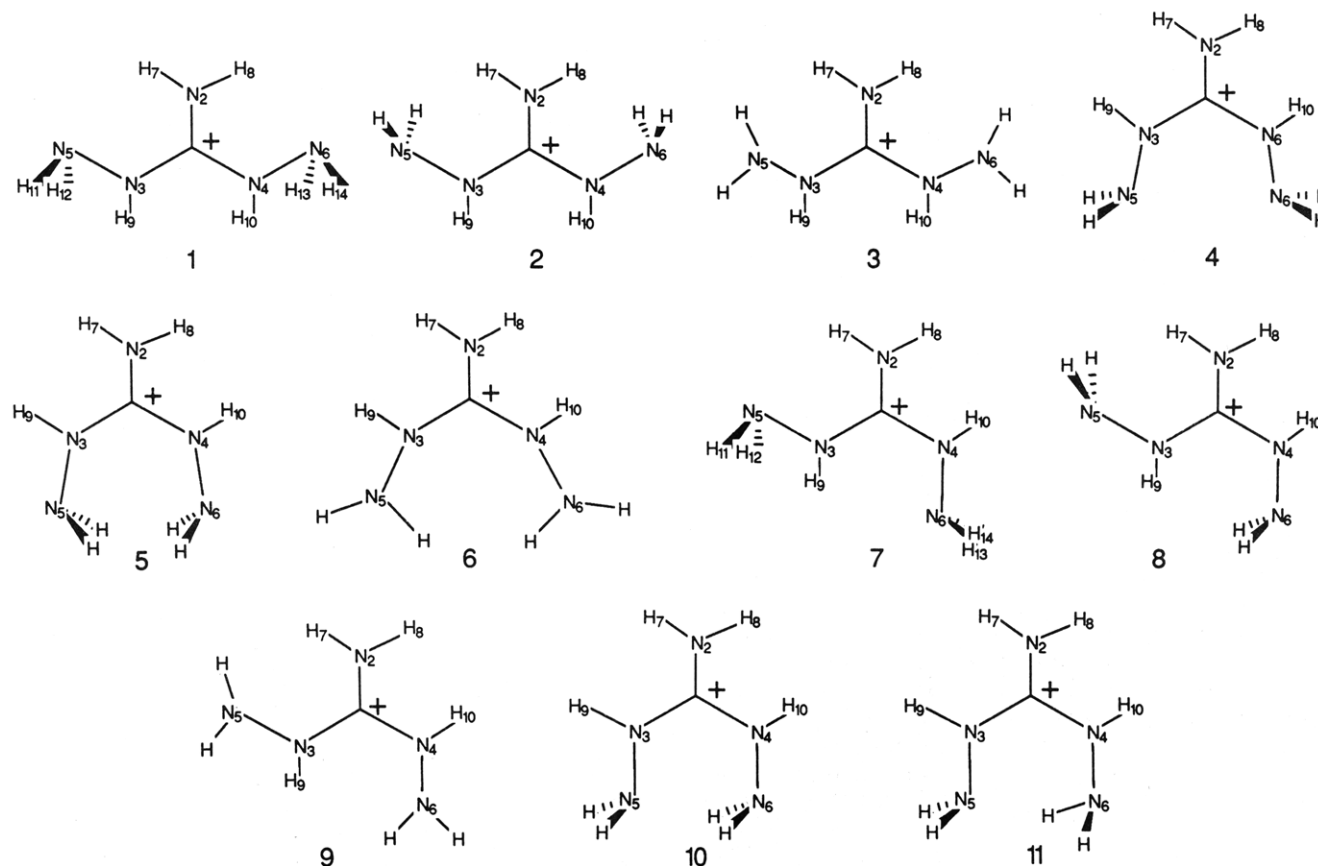


**Figure 2.** Stereodrawing of the unit cell for diaminoguanidinium nitrate. The origin is at the lower right. Hydrogen bonds are dotted.

**Chart I. Possible Conformations of the Diaminoguanidinium Cation**



in the asymmetric unit. A stereodrawing of the unit cell is shown in Figure 2. With the exception of the hydrogen atoms on the two terminal groups, the DAG cation is approximately planar (within 0.08 Å). Five of the hydrogens are involved in N-H...O hydrogen bonds.

The conformation of the cation differs in the DAGNIT and DAGNTO salts, although both cations have similar bond lengths and are approximately planar. Figure 3 shows the asymmetric unit of DAGNTO, while Figure 4 shows a stereodrawing of the unit cell. In DAGNTO, the cation has approximate  $S_v$  symmetry with both of the central amino group hydrogen atoms directed toward the lone-pair regions of the terminal amino groups. In DAGNIT, there has been a 180° rotation about the C-N(4) bond so that only one of the central hydrogen atoms, H(4), is directed toward a lone-pair region.

**Single Molecule Energies.** To help understand why the two observed structures (DAGNTO corresponding to structure 1 and DAGNIT corresponding to structure 7 in Chart I) might be preferred, we have examined these various structures with several levels of calculation. Results of calculations for the species shown in Chart I are summarized in Table II. Bond lengths and bond angles

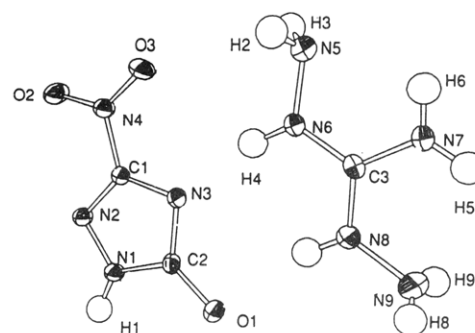


**Figure 3.** ORTEP drawing of the asymmetric unit of DAGNTO. Thermal ellipsoids are 50% probability.

from the X-ray analysis are also included for comparison. Table III shows the relative energies and number of negative force constants of the DAG conformers as calculated using the indicated theoretical model.

AM1 calculations give isomers 1 and 7 as the two most stable forms. They are of nearly equal energy, with 7 being favored by only 0.3 kcal/mol. Structures 2, 4, 5, 8, and 10 form a related second set, lying up to 8 kcal/mol higher

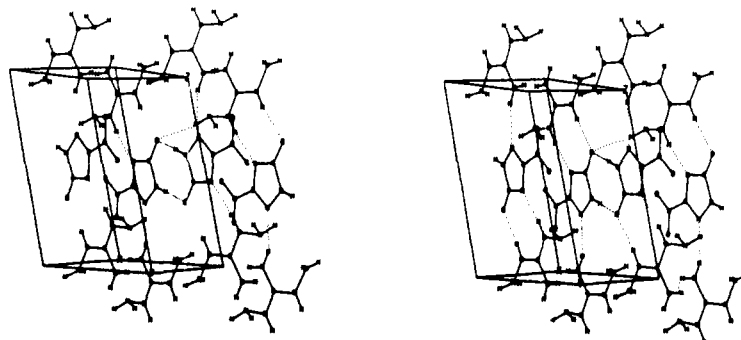


**Figure 4.** Stereodrawing of the unit cell in DAGNTO. The origin is at the lower right. Hydrogen bonds are dotted.

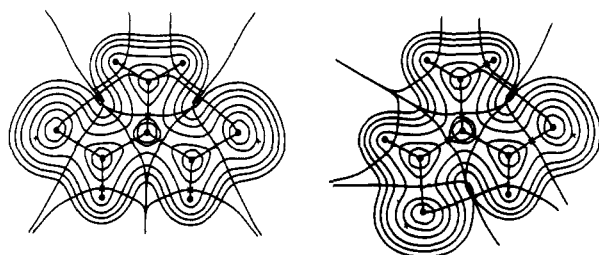


**Figure 5.** Plots of the calculated electron density, bond paths, and interatomic surfaces in the heavy atom plane. The cation in DAGNTO appears on the left, while that of DAGNIT appears on the right. Electron density contours occur at 0.02, 0.04, 0.08, 0.2, 0.4, 0.8 e/au<sup>3</sup>. Atom positions in the plane are indicated by heavy circles, while projected atom positions are indicated by pluses. Bond points are indicated with asterisks (\*) and ring critical points are indicated with unfilled circles.

in energy. These structures differ from 1 and 7 by inversion of one or both of the terminal amino groups. A third set of structures (3, 6, and 9) lie 30–65 kcal/mol above 1. These structures contain planar terminal amino groups, which are apparently highly unfavorable energetically. Attempts to locate a structure corresponding to 11 always reverted to 10 with AM1.

Force constant calculations using AM1, which are summarized in Table III, are somewhat puzzling, but can be understood with additional considerations. According to AM1, not one of the species in Chart I corresponds to a potential energy minima. In all cases, however, some or all of the negative force constants corresponded to out of plane motions of the N<sub>3</sub> and N<sub>4</sub> nitrogens. Symmetric and asymmetric combinations of this motion leads to two modes. We have previously found that AM1 overestimates the pyramidal-planar nitrogen energy differences in other contexts; thus, as many as two negative force constants may arise as a result of this artifact. By ignoring the modes associated with these negative force constants, 1, 2, 5, 7, 8, and 10 would then represent potential energy minima. The additional negative mode in 4 corresponds to an asymmetric simultaneous rotation about the C–N bonds. Structures 3, 6, and 9 both possess several additional unstable vibrational modes and are relatively high in energy.

The results of ab initio calculations are also summarized in Tables II and III. At both 3-21G and 6-31G\*, 7 is found to be of lowest energy, with 1 slightly higher, as in the AM1 calculations. At 3-21G, 5, 10, and 11 are found to be of even higher energy, but by a considerably larger amount than in the AM1 calculations. Structure 11 appears to possess an internal hydrogen bond between the terminal amino groups. Comparison of the relative energies obtained at 3-21G and 6-31G\* show only a small effect of basis set size.

Force constant calculations at 3-21G verified 1 and 7 as minima in the potential energy surface. In contrast, 5 was found to be a hilltop, possessing two vibrational modes leading to a decrease in the energy. A single negative force constant was found for 10. Displacement along the associated normal mode, followed by complete optimization, resulted in 11. This structure was found to be a local minimum, possessing no negative force constants.

**Topological Analysis.** Figure 5 illustrates contour maps of the electron distribution for 1 and 7 as obtained from the 6-31G\* calculations. Superimposed upon the maps are the interatomic surfaces, through which no gradient paths pass, and the bond paths, which link together the atoms of the molecule. In addition to the expected bond paths, corresponding with traditional notions of bonds as illustrated in Chart I, there appear additional, unexpected paths. In the W form, these paths link the N of the terminal NH<sub>2</sub> groups to the N of the central NH<sub>2</sub> group. In the S form, one of these paths links the N of a terminal NH<sub>2</sub> group to the N of the central NH<sub>2</sub> group, and the other path links the N of the remaining terminal NH<sub>2</sub> group to the N of the NH grouping. Thus, rather than a path linking N to H, as would be expected for a typical hydrogen bond, paths appear linking the heavy atoms involved. A similar absence of a bond path where an H bond is anticipated occurs in protonated fluoroacetone,<sup>20</sup> where a bond path linking F and O is found, rather than one linking F–H. Further analysis is required to determine the reasons for these observations.

Calculated values of the ellipticity ( $\epsilon$ ), electron density ( $\rho_c$ ), and  $\nabla^2\rho_c$  at the critical points in the electron density are found in Table IV. Bond points surrounding C<sub>1</sub> are found to have values of larger magnitude for the quantities  $\epsilon$ ,  $\rho_c$ , and  $\nabla^2\rho_c$  than for bond points between nitrogen atoms. These values are reasonably similar for the W and S forms, and show noncylindrically symmetric bonds between the bonded atoms.

Shown in Table V are the integrated total electron populations of each of the topological atoms. Integrated  $\pi$  populations are also shown for those atoms which may change in important resonance forms. These total populations show carbon bearing a charge greater than +2, while the adjacent nitrogens bear charges of over –1, and the terminal nitrogens bear a charge of  $\sim -0.7$ . Although these values may seem quite large, examination of the  $\pi$  populations shows a more familiar pattern. Carbon bears about 0.4 e in its  $\pi$  orbital, while the adjacent nitrogens show small deficits compared with 2 e expected for a completely localized charge distribution. These results support the

(20) Choi, S. C.; Boyd, R. J. *Can. J. Chem.* 1986, 64, 2042.

(21) Bader, R. F. W.; Tang, T.-H.; Tal, Y.; Biegler-Kong, R. W. *J. Am. Chem. Soc.* 1982, 104, 946.

(22) Bader, R. F. W.; Essen, H. *J. Chem. Phys.* 1984, 80, 1943.

**Table II. Calculated Energies<sup>a</sup> and Heavy Atom Bond Lengths and Angles in Diaminoguanidinium Cation for the Indicated Structures (Numbering from Chart I)**

	X-ray	AM1	3-21G	6-31G*			
<b>1</b>							
energy		208.2	-312.78369	-314.51739			
$R(\text{C}-\text{N}_2)$	1.320	1.361	1.304	1.307			
$R(\text{C}-\text{N}_3)$	1.329	1.403	1.334	1.331			
$R(\text{C}-\text{N}_4)$	1.320	1.403	1.334	1.331			
$R(\text{N}_4-\text{N}_6)$	1.401	1.360	1.421	1.386			
$R(\text{N}_5-\text{N}_7)$	1.410	1.360	1.421	1.386			
$\angle \text{N}_2\text{CN}_3$	120.6	121.8	118.8	120.6			
$\angle \text{N}_2\text{CN}_4$	120.0	121.8	118.8	120.6			
$\angle \text{CN}_2\text{N}_4$	120.4	120.5	120.4	119.0			
$\angle \text{CN}_3\text{N}_5$	117.9	120.5	120.4	119.0			
		AM1					
		2	3	4	6	8	9
energy	213.0	239.1	215.9	243.6	212.9	239.1	
$R(\text{C}-\text{N}_2)$	1.374	1.378	1.383	1.394	1.373	1.384	
$R(\text{C}-\text{N}_3)$	1.396	1.391	1.391	1.383	1.396	1.386	
$R(\text{C}-\text{N}_4)$					1.397	1.392	
$R(\text{N}_3-\text{N}_5)$	1.349	1.345	1.358	1.340	1.350	1.345	
$R(\text{N}_4-\text{N}_6)$					1.349	1.344	
$\angle \text{N}_2\text{CN}_3$	121.0	122.1	117.2	116.2	121.0	122.1	
$\angle \text{N}_2\text{CN}_4$					118.8	117.1	
$\angle \text{CN}_2\text{N}_4$	128.4	126.0	123.7	130.2	128.6	127.1	
$\angle \text{CN}_3\text{N}_5$					128.3	125.8	
			AM1	3-21G			
<b>5</b>							
energy			214.5	-312.74631			
$R(\text{C}-\text{N}_2)$			1.374	1.333			
$R(\text{C}-\text{N}_3)$			1.396	1.327			
$R(\text{N}-\text{N})$			1.346	1.399			
$\angle \text{NCN}$			118.4	117.1			
$\angle \text{CNN}$			130.0	127.7			
			X-ray	AM1	3-21G	6-31G*	
<b>7</b>							
energy			207.9	-132.78526	-314.51830		
$R(\text{C}-\text{N}_2)$	1.323	1.370	1.316	1.317			
$R(\text{C}-\text{N}_3)$	1.323	1.393	1.322	1.321			
$R(\text{C}-\text{N}_4)$	1.326	1.403	1.333	1.331			
$R(\text{N}_3-\text{N}_5)$	1.415	1.362	1.421	1.388			
$R(\text{N}_4-\text{N}_6)$	1.407	1.360	1.422	1.387			
$\angle \text{N}_2\text{CN}_3$	120.4	121.9	120.0	120.4			
$\angle \text{N}_2\text{CN}_4$	119.9	118.2	121.1	120.3			
$\angle \text{CN}_3\text{N}_5$	119.0	120.7	117.6	119.1			
$\angle \text{CN}_4\text{N}_6$	118.9	121.2	117.4	119.3			
<b>10</b>							
energy			209.2	-312.75600			
$R(\text{C}-\text{N}_2)$			1.377	1.366			
$R(\text{C}-\text{N}_3)$			1.398	1.330			
$R(\text{C}-\text{N}_4)$			1.390	1.320			
$R(\text{N}_3-\text{N}_5)$			1.350	1.421			
$R(\text{N}_4-\text{N}_6)$			1.358	1.432			
$\angle \text{N}_2\text{CN}_3$			117.7	116.9			
$\angle \text{N}_2\text{CN}_4$			118.6	117.5			
$\angle \text{CN}_3\text{N}_5$			122.2	122.4			
$\angle \text{CN}_4\text{N}_6$			130.5	130.2			
<b>11</b>							
energy			-312.75800	-314.49611			
$R(\text{C}-\text{N}_2)$			1.333	1.329			
$R(\text{C}-\text{N}_3)$			1.333	1.330			
$R(\text{C}-\text{N}_4)$			1.318	1.319			
$R(\text{N}_3-\text{N}_5)$			1.425	1.390			
$R(\text{N}_4-\text{N}_6)$			1.430	1.390			
$\angle \text{N}_2\text{CN}_3$			117.4	117.7			
$\angle \text{N}_2\text{CN}_4$			118.4	118.4			
$\text{CN}_3\text{N}_5$			121.2	122.0			
$\angle \text{CN}_4\text{N}_6$			127.7	128.7			

<sup>a</sup> Energies for AM1 calculations are heats of formation in kilocalories/mole and for ab initio calculations are absolute energies in hartrees.

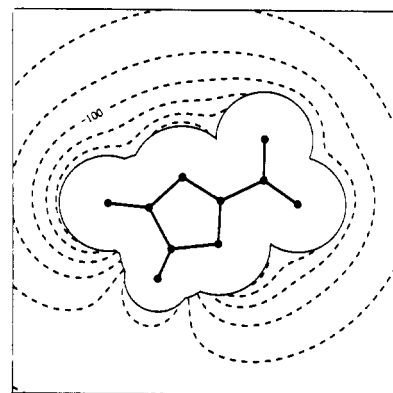


**Figure 6.** Calculated electrostatic potential (kcal/mol/e) of the conjugate base of NTO. Negative values are represented by dashed lines, and zero by combination dash-dot lines.

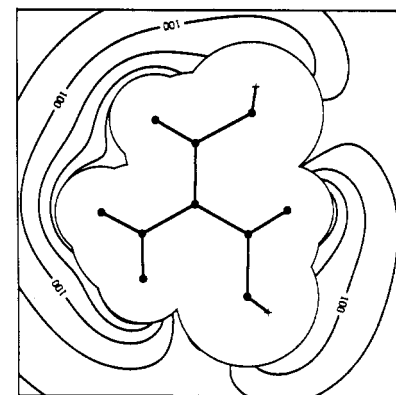
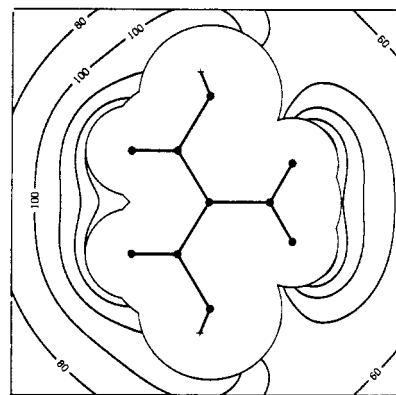


**Figure 7.** Calculated electrostatic potential (kcal/mol/e) of diaminoguanidinium cation in the two conformations.

standard models of charge delocalization by resonance interactions.

**Electrostatic Calculations.** To determine qualitatively what geometries the DAGNTO salts might assume, the electrostatic potentials of the W and S forms as well as that of the conjugate base of NTO were calculated. As shown in Figure 6, the most negative sites in the conjugate base occur on the 4-nitrogen and on the carbonyl oxygen. Figure 7 shows the results for the two forms of DAG. The most positive regions of these cations are associated with one of the  $=\text{NH}_2$  hydrogens and one of the NH hydrogens

**Table III. Calculated Relative Energies (kcal/mol)<sup>a</sup>**

method	1	2	3	4	5	6	7	8	9	10	11
AM1	0.3 (2)	5.1 (1)	31.2 (7)	8.0 (3)	6.6 (2)	35.7 (7)	0.0 (2)	5.0 (2)	31.2 (7)	1.3 (2)	-
3-21G	1.0 (0)				24.5 (2)		0.0 (0)			18.4 (1)	17.1 (0)
6-31G*	0.6						0.0				13.9

<sup>a</sup> When calculated, the number of negative force constants found are indicated in parentheses following the relative energy.

Table IV. Critical Point Properties As Determined Using the 6-31G\* Results<sup>a</sup>

		$\lambda_1$	$\lambda_2$	$\lambda_3$	$\epsilon_c$	$\rho_c$	$\nabla^2\rho_c$
C <sub>1</sub> -N <sub>3</sub>	W	-0.966	-0.861	0.652	0.122	0.377	-1.175
	S	-0.932	-0.847	0.618	0.101	0.368	-1.161
C <sub>1</sub> -N <sub>2</sub>	W	-0.914	-0.827	0.570	0.106	0.361	-1.172
	S	-0.949	-0.842	0.601	0.127	0.370	-1.190
C <sub>1</sub> -N <sub>4</sub>	W	-0.915	-0.827	0.570	0.106	0.361	-1.172
	S	-0.915	-0.828	0.571	0.106	0.361	-1.172
N <sub>2</sub> -N <sub>1</sub>	W	-0.739	-0.697	0.688	0.060	0.339	-0.748
	S	-0.741	-0.701	0.689	0.057	0.340	-0.754
N <sub>4</sub> -N <sub>5</sub>	W	-0.739	-0.697	0.688	0.060	0.339	-0.748
	S	-0.739	-0.700	0.689	0.056	0.340	-0.751
N <sub>1</sub> -N <sub>3</sub>	W	-0.018	-0.005	0.109	2.88	0.019	0.086
	S	-0.019	-0.008	0.112	1.47	0.019	0.085
N <sub>5</sub> -N <sub>2</sub>	S	-0.020	-0.012	0.115	0.71	0.020	0.083
	W	-0.017	0.005	0.108		0.018	0.097
ring points	S	-0.017	0.010	0.111		0.019	0.104
	S'	-0.017	0.017	0.112		0.019	0.112

<sup>a</sup>Quantities are in atomic units. Curvatures ( $\lambda_1, \lambda_2, \lambda_3$ ) are eigenvalues of the second derivative matrix of the electron density with respect to the cartesian coordinates. The ellipticity ( $\epsilon$ ) is defined as  $\epsilon = (\lambda_1/\lambda_2) - 1$  and represents the deviation of the electron density from cylindrical symmetry at the critical point. Values of the electron density ( $\rho_c$ ) and the Laplacian of the electron density ( $\nabla^2\rho_c$ ) are also shown.

Table V. Electron Populations Obtained from Integration of the Atomic Volumes in 1 and 7

	$n_{tot}$	$n_x$	$n_{tot}$
1	C <sub>1</sub> : 3.682	0.416	H <sub>8</sub> : 0.464
	N <sub>2</sub> : 8.503	1.810	H <sub>10</sub> : 0.523
	N <sub>4</sub> : 8.110	1.842	H <sub>12</sub> : 0.556
	N <sub>6</sub> : 7.699		
7	C <sub>1</sub> : 3.666	0.412	H <sub>7</sub> : 0.460
	N <sub>2</sub> : 8.456	1.832	H <sub>8</sub> : 0.502
	N <sub>3</sub> : 8.170	1.836	H <sub>9</sub> : 0.478
	N <sub>4</sub> : 8.111	1.844	H <sub>10</sub> : 0.519
	N <sub>5</sub> : 7.703		H <sub>11</sub> : 0.557
	N <sub>6</sub> : 7.705		H <sub>13</sub> : 0.555

in the S form. In the W form, the two NH groups are most positive. Simply aligning the most positive regions of this cation with the most negative regions on the anion results in a qualitative geometry for the DAGNTO salt similar to that found experimentally, as illustrated in Figure 3.

More quantitative results can be obtained by calculating the electrostatic interaction between the two most stable forms of DAG and the anion. The intermolecular separations were varied to provide the lowest energy, as described in the Methods section, above. Figure 8 shows the minimum energy configurations found for the NTO/DAGW and NTO/DAGS ion pairs. Many other structures were investigated, but these are the lowest energy forms found. As expected, the two structures are very similar in their hydrogen-bonding interactions with the two NH moieties of the DAG directed toward the carbonyl oxygen and the 4-nitrogen of NTO. In both cases, the DAG molecules are skewed toward the oxygen of the nitro group, which is also has large negative potentials associated with it. Both complexes were found to be planar, although they were not constrained to be so.

The NTO/DAGW complex was found to be 3.4 kcal/mol more stable than the NTO/DAGS complex. Comparison of Figure 7, parts a and b, shows that, in the W form, the bonding hydrogens are more positive than the corresponding hydrogens in the S form. This feature leads to more favorable interactions between DAGW and the anion than for the other isomer. Since the difference in energy between the two complexes is larger than the difference in energy of the isolated molecules, as shown by single-molecule calculations described above, it is the electrostatic energy which selectively allows the conjugate base of NTO to bind DAGW.

A comparison between our calculated structure for the NTO/DAGW complex and the asymmetric unit deter-

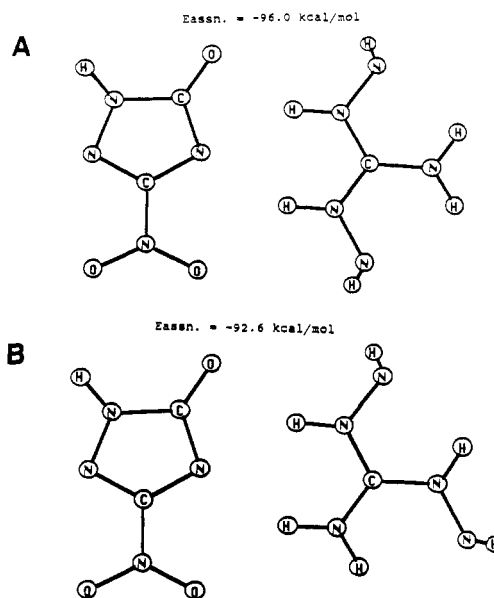


Figure 8. Lowest energy configurations of the NTO/DAGW (A) and NTO/DAGS (B) anion/cation complexes. Total calculated association energies as shown.

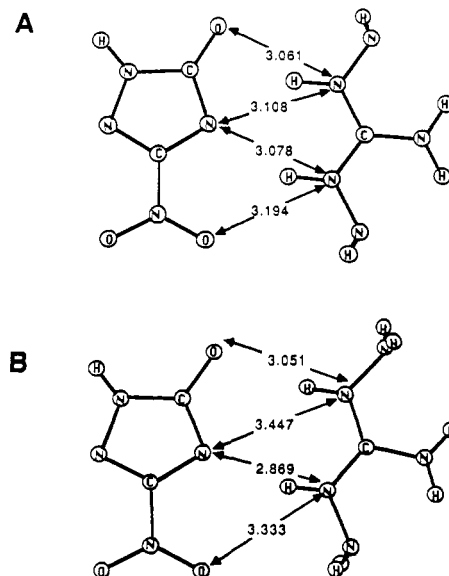
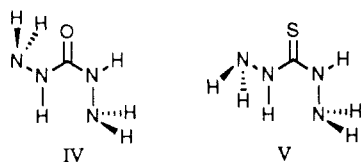


Figure 9. Comparison of some intermolecular distances as found from the calculations (A) and in the X-ray structure (B).

mined by X-ray crystallography is shown in Figure 9. The electrostatic model is seen to reproduce the observed structure at least qualitatively.

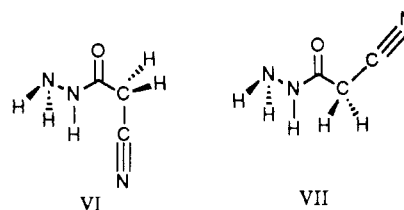
### Discussion

The above results demonstrate that molecular conformation may differ in the gas and condensed phases. Other investigations comparing the "free" and crystal geometries of conformationally floppy molecules have been performed. Crystal structure determinations of carbonylhydrazide (IV)<sup>23</sup> and thiocarbonylhydrazide (V)<sup>24</sup> show that they adopt the indicated conformations, which are different. Although no theoretical analysis was found for V, molecular orbital calculations indicate IV to be the lowest energy conformation.<sup>25</sup> Thus, no special considerations due to the crystal environment are needed to rationalize its observed structure, and the molecule is inferred to have the same conformation in both the gas and condensed phases.



A comparison of calculated structures with that found in the (neutron) crystal of  $\alpha$ -cyanoacetohydrazide has also been performed.<sup>26</sup> For this compound, HF/3-21G and HF/6-31G\* calculations predict VI to be most stable with VII lying 8.75 kcal/mol higher in energy (HF/6-31G\*). Nonetheless, a somewhat distorted version of VII is the conformation observed in the crystal structure. The presence of a high-energy conformation in the condensed phase was attributed to self-association, via an extensive network of hydrogen bonds.

DAG is a charged species and will also interact very strongly with other molecules in the crystal, especially



nearest-neighbor anions. Our electrostatic calculations for the DAGNTO complex show that energy differences of a single anion/cation pair can rationalize the observed results. In this particular case, we think this limited analysis is significant because the extended structure consists of linked ribbons of the DAGNTO unit. In general, however, there may exist no unique way of choosing such a small unit for analysis, and the problem becomes one of accounting for different molecular conformations in crystal structure calculations. A particular example of this is the DAGNIT salt where the nitrate anion hydrogen bonds to many different DAG cations and no simple dimer or even tetramer could properly include all important interactions. Such a problem will be quite complex in general.

### Conclusions

The diaminoguanidinium (DAG) cation undergoes conformational interconversions under conditions of salt formation. As a result, it appears in two different forms in its salt with the nitrate ion and the conjugate base of 3-nitro-1,2,4-triazol-5-one (NTO). Favorable electrostatic interaction of one of the DAG forms with the NTO conjugate base lead to its selective binding, despite the presence of another form of competitive "free" energy. The Bader analysis suggests that the conformations in the DAG cations is controlled, not by hydrogen bonds, but by lone pair-heavy atom interactions. Traditional ideas of resonance stabilization, especially Y-delocalization,<sup>27</sup> were supported by the charge distribution analysis.

**Registry No.** II-III, 10308-83-5.

**Supplementary Material Available:** Tables of crystallographic and calculated coordinates (9 pages); table of structure factors (4 pages). Ordering information given on any current masthead page.

(23) (a) Domiano, P.; Pellinghelli, M. A.; Tiripicchio, A. *Acta Crystallogr.* **1972**, *B28*, 2495. (b) Ottersen, T.; Hope, J. *Acta Crystallogr.* **1979**, *B35*, 373.

(24) Braibanti, A.; Tiripicchio, A.; Camellini, M. T. *Acta Crystallogr.* **1969**, *B25*, 2286.

(25) Jeffrey, G. A.; Ruble, J. R.; Nanni, R. G.; Turano, A. M.; Yates, J. H. *Acta Crystallogr.* **1985**, *B41*, 354.

(26) Nanni, R. G.; Ruble, J. R.; Jeffrey, G. A.; McMullan, R. K. *J. Mol. Struct.* **1986**, *147*, 369.

(27) Gund, P. *J. Chem. Educ.* **1972**, *49*, 100.